

# State Estimation Methods in Navigation: Overview and Application

**Jindřich Duník, University of West Bohemia**

**Sanat K. Biswas, Indian Institute of Technology Delhi**

**Andrew G. Dempster, UNSW Sydney**

**Thomas Pany, Universität der Bundeswehr München**

**Pau Closas, Northeastern University**

## INTRODUCTION TO BAYESIAN STATE ESTIMATION

The *state* of a *system* is a variable, which fully characterizes the status of the system at a given time. Knowledge of the state is, thus, essential for control or prediction of the system's future behavior. Unfortunately, the state of the system is typically not directly measurable, i.e., it is not known. Instead, the state is indirectly observed via *measurement* only which is somehow related to the state. The measurements are, moreover, affected by the noise.

State estimation of stochastic dynamic systems deals with the estimation of the time-varying state from noisy measurements. State estimation has been a subject of considerable research interest for more than five decades.<sup>1</sup> Although its development was motivated by the needs of tracking and navigation applications, state estimation these days plays an indispensable role also in many other technical and nontechnical fields such as automatic

control, speech and image processing, biology, economy, weather forecasting, etc., [1], [2].

The goal of this article is to introduce selected methods of the state estimation, which are used in navigation applications. In particular, the article is focused on *navigation* applications, which belong into the area of expertise of the IEEE AESS Navigation Systems Panel<sup>2</sup> (NSP), of which the authors are members.

The article is organized as follows. In the rest of this section, state-space modeling and Bayesian state estimation are briefly reviewed. In the sections “State Estimation Methods: An Overview” and “State Estimation Methods: Additional Topics,” an overview of state estimation methods, related terminology, and algorithms is given with stress on topics relevant to NSP technologies. Selected state-of-the-art applications falling within the scope of the NSP are then described and discussed with emphasis on sensor error sources in “Estimation in Navigation Systems.” Finally, concluding remarks are given.

<sup>1</sup>State estimation is a part of a general estimation theory of which development can be dated back to the beginning of 19th century. The development started with a design of the least-squares method by C. F. Gauss and A.-M. Legendre and it was motivated by modeling planetary motion [1].

Authors' current addresses: J. Duník, University of West Bohemia, Pilsen 30100, Czech Republic (e-mail: dunikj@kky.zcu.cz). S. K. Biswas, Indian Institute of Technology Delhi, Delhi 110016, India. A. G. Dempster, UNSW Sydney, Sydney, NSW 2052, Australia. T. Pany, Universität der Bundeswehr München, 85579 Neubiberg, Germany. P. Closas, Northeastern University, Boston, MA 02115, USA.

Manuscript received December 2, 2019, revised April 15, 2020, May 20, 2020, and ready for publication June 10, 2020.

Review handled by Peter Willett.  
0885-8985/20/\$26.00 © 2020 IEEE

## SYSTEM STATE-SPACE MODEL

State estimation methods provide the state estimate on the basis of the available measurements and a known state-space model. In this article, the following discrete-time nonlinear stochastic dynamic state-space model with additive noises

$$\mathbf{x}_{k+1} = \mathbf{f}_k(\mathbf{x}_k, \mathbf{u}_k) + \mathbf{w}_k \quad (1)$$

$$\mathbf{z}_k = \mathbf{h}_k(\mathbf{x}_k) + \mathbf{v}_k \quad (2)$$

is considered, where the vector  $\mathbf{x}_k \in \mathbb{R}^{n_x}$  represents the *unknown* state of the system at time instant  $k$ , the vectors  $\mathbf{u}_k \in \mathbb{R}^{n_u}$  and  $\mathbf{z}_k \in \mathbb{R}^{n_z}$  represent the *known* input and measurement at time instant  $k$ , the functions  $\mathbf{f}_k : \mathbb{R}^{n_x} \times \mathbb{R}^{n_u} \rightarrow \mathbb{R}^{n_x}$  and  $\mathbf{h}_k : \mathbb{R}^{n_x} \rightarrow \mathbb{R}^{n_z}$  are *known* state and

<sup>2</sup>The NSP webpage is <http://ieee-aess.org/tech-ops/navigation-systems-panel>

measurement nonlinear vector transformations, and the vectors  $\mathbf{w}_k$ ,  $\mathbf{v}_k$  represent unknown state and measurement noises with *known* descriptions in the form of the probability density functions (PDFs)  $p(\mathbf{w}_k)$ ,  $p(\mathbf{v}_k)$ , respectively.

The initial state PDF  $p(\mathbf{x}_0)$  is *known* and independent of the noises. The state equation (1) models time behavior of the state and the measurement equation (2) gives a relation between the sought state and available measurement.

In navigation applications, the *system* may refer to a navigated vehicle, the *state*  $\mathbf{x}_k$  to sought vehicle navigation information (i.e., vehicle position, velocity, attitude, and heading), the *input*  $\mathbf{u}_k$  to, e.g., the readings of an inertial measurement unit (IMU), and the *measurement*  $\mathbf{z}_k$ , e.g., to the readings of a global navigation satellite system (GNSS) receiver. Then, the nonlinear function  $\mathbf{f}_k(\cdot)$  in (1) stems from dynamic or kinematic laws,  $\mathbf{h}_k(\cdot)$  in (2) models a relation between the receiver output and state variables, and the state and measurement noise PDFs  $p(\mathbf{w}_k)$ ,  $p(\mathbf{v}_k)$  are determined by the noise properties of the IMU and GNSS receiver [3], [4].

## STATE ESTIMATION AND BAYESIAN RECURSIVE RELATIONS

The goal of state estimation, or more precisely filtering, is to find an estimate of the state  $\mathbf{x}_k$  on the basis of a sequence of all measurements  $\mathbf{z}^k = [\mathbf{z}_0, \mathbf{z}_1, \dots, \mathbf{z}_k]$  up to the time instant  $k$  and the model (1), (2). In particular, in the *Bayesian* formulation of state estimation, the goal is to

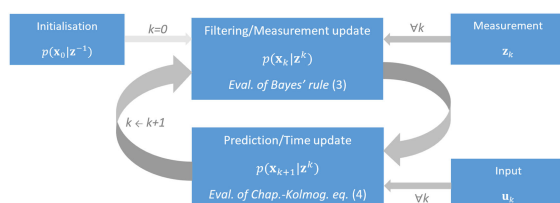


**Figure 1.**  
Illustration of the Bayesian recursion.

find the PDF of the state  $\mathbf{x}_k$  conditioned on the measurements  $\mathbf{z}^k$ , i.e., the estimate in the form of the conditional PDF  $p(\mathbf{x}_k|\mathbf{z}^k)$ ,  $\forall k$ , is sought. The conditional PDF provides a full description of the state estimate.

In the Bayesian framework, the general solution for state estimation is given by the Bayesian recursive relations (BRRs) for the computation of the conditional PDFs,<sup>3</sup> [5]

$$p(\mathbf{x}_k|\mathbf{z}^k) = \frac{p(\mathbf{x}_k|\mathbf{z}^{k-1})p(\mathbf{z}_k|\mathbf{x}_k)}{p(\mathbf{z}_k|\mathbf{z}^{k-1})} \quad (3)$$

$$p(\mathbf{x}_{k+1}|\mathbf{z}^k) = \int p(\mathbf{x}_{k+1}|\mathbf{x}_k)p(\mathbf{x}_k|\mathbf{z}^k)d\mathbf{x}_k \quad (4)$$

where  $p(\mathbf{x}_k|\mathbf{z}^k)$  is the filtering PDF computed by Bayes' rule (3) and  $p(\mathbf{x}_k|\mathbf{z}^{k-1})$  is the one-step predictive PDF computed by the Chapman-Kolmogorov equation (4). The PDFs  $p(\mathbf{x}_{k+1}|\mathbf{x}_k)$  and  $p(\mathbf{z}_k|\mathbf{x}_k)$  are the state transition PDF and measurement PDF unequivocally obtained from the model (1) and (2), respectively. The PDF

$$p(\mathbf{z}_k|\mathbf{z}^{k-1}) = \int p(\mathbf{x}_k|\mathbf{z}^{k-1})p(\mathbf{z}_k|\mathbf{x}_k)d\mathbf{x}_k \quad (5)$$

is the one-step predictive PDF of the measurement. The Bayesian recursion (3), (4) starts from the system's initial condition  $p(\mathbf{x}_0|\mathbf{z}^{-1}) = p(\mathbf{x}_0)$ . The Bayesian recursion is illustrated in Figure 1.

## STATE ESTIMATION METHODS: AN OVERVIEW

The BRRs are complex functional relations about which *exact* solution is possible for a limited set of models only. In other cases, an approximate solution to the BRRs must be employed. These approximate methods can be divided,

<sup>3</sup>Considering the model (1), (2), the BRRs (3), (4) should be conditioned also on *available* sequence of the input  $\mathbf{u}_k, \forall k$ . However, for the sake of notational simplicity, the input signal is assumed to be implicitly part of the condition and it is not explicitly stated, i.e.,  $p(\mathbf{x}_{k+1}|\mathbf{x}_k) = p(\mathbf{x}_{k+1}|\mathbf{x}_k; \mathbf{u}_k)$ ,  $p(\mathbf{x}_k|\mathbf{z}^k) = p(\mathbf{x}_k|\mathbf{z}^k; \mathbf{u}^{k-1})$ , and  $p(\mathbf{x}_{k+1}|\mathbf{z}^k) = p(\mathbf{x}_{k+1}|\mathbf{z}^k; \mathbf{u}^k)$ .

with respect to validity of the estimates, into *local* and *global* methods [6]–[8].

## EXACT METHODS

The exact methods have been typically designed for a set of the linear models. For this set, the solution to the BRRs results in *reproducible* conditional PDFs, i.e., the conditional PDFs at subsequent time instants share the same distribution and, thus, recursive conditional PDF computation reduces to recursive computation of conditional PDF parameters only. The exact methods are represented, e.g., by the Kalman filter (KF) or the Gaussian sum filter (GSF) [5], [94]. The KF, developed in the sixties, is an optimal<sup>4</sup> estimator for the linear Gaussian models, i.e., for the linear model (1), (2) with the state noise, measurement noise, and the initial condition described by Gaussian PDFs. The recursive solution to the functional BRRs then collapses to the recursive computation of the conditional mean and covariance matrices only, which fully describe the Gaussian conditional PDFs. The GSF is an optimal estimator for the linear Gaussian sum models and can be imagined as a bank of concurrently running KFs [94]. Consequently, the conditional PDFs are in the form of Gaussian sums and the solution of the BRRs, then, lies in computation of the weights, means, and covariance matrices of the particular terms of the Gaussian sum conditional PDF.

## LOCAL METHODS

Local methods are based on two approximations; first, the joint conditional predictive state and measurement PDF is assumed to be Gaussian; second, the nonlinear functions in (1) and (2) are linearized. The former approximation results in a *linear* structure of a local filter (LF) with respect to the measurement, and, together with the latter approximation, it allows use of the (linear) KF design technique also for nonlinear models. All LFs, therefore, share the same algorithm structure, but they differ in which linearization of the nonlinear functions in (1) and (2) is used. In particular, two different types of linearization can be found in the literature: derivative-based and derivative-free.

The *derivative-based* LFs, developed in the seventies, approximate the nonlinear function by the Taylor expansion (TE). Whereas utilization of the first-order TE leads to the extended Kalman filter (EKF) or the linearized KF (depending on the selection of the linearization point) [5], [9], approximation based on the second-order TE results in the second-order filter (SOF). In the literature, several versions of the SOF have been proposed [9], [10], [12] and, also, utilization of a higher order TE in the LF design has been discussed [13].

<sup>4</sup>The term “optimal” is, in this article, related to the exact solution to the BRR.

The *derivative-free* LFs appeared at the beginning of the century. They are based either on a polynomial expansion of the nonlinear functions or on the approximation of the state estimate by a weighted set of deterministically or stochastically selected points. The former approximation in the LF design is represented by Stirling’s interpolation (SI) of the first or second order, which results in the divided difference filters of the first or second order (DD1, DD2), respectively [14], [15]. The SI can be understood as the TE, where derivatives are substituted with differences [8]. The latter approximation takes advantage of a different idea, where the nonlinear function is preserved, but the conditional (Gaussian-assumed) PDF is approximated by a set of points. This approximation is represented by the unscented transformation<sup>5</sup> (UT) [2], [9], [16], deterministic quadrature and cubature integration rules [7], [11], [17]–[19], and stochastic integration rules [20], which results in the set of the LFs including the unscented Kalman filter (UKF), cubature Kalman filter, the stochastic integration filter, or the ensemble Kalman filter. Note that last mentioned filter, propagating the set of randomly drawn samples instead of the moments, is a suitable algorithm for a high-dimensional state-space model [20], [98]. It is worth noting that although the point-based approximations use a different basic idea, they can be interpreted as examples of the statistical *linear* regression of the nonlinear functions [8], [21].

Examples of approximation of a *scalar* nonlinear function  $f_k(x_k)$  by the derivative-based first-order TE and the derivative-free first-order Stirling’s interpolation are shown in Figure 2. It can be seen that the TE-based linearization  $\hat{f}_k(x_k; \hat{x}_k)$  is more accurate in a close vicinity of the linearization point  $\hat{x}_k$ , whereas the SI-based is better in the wider vicinity. The reason can be found in the fact that the derivative-free approximation is computed over an interval defined by the set of (transformed) points.

Independent of which nonlinear function approximation is used, all the LFs provide estimates in the form of the first two moments of an *approximate* Gaussian conditional PDF, i.e., in the form of the conditional mean and covariance matrix. The moments do not represent a full description of the immeasurable state and are valid if and only if the filter is working in the close vicinity of the true state (thus, the name *local*), which is, however, not known in practice. Therefore, significant attention has been devoted to the theoretical analysis and monitoring of the conditions under which a LF provides accurate<sup>6</sup> and

<sup>5</sup>The UT should be understood as a class of approximations rather than one single approach. In the literature, various versions of the UT have been proposed with different strategies to point selection [16].

<sup>6</sup>The LFs can be divided into first-order filters (e.g., the EKF, DD1) and SOFs (e.g., the SOF, DD2, UKF). The latter are expected to provide more accurate estimates, but it is not a rule (due to unknown impact of neglected terms in the nonlinear function approximation).

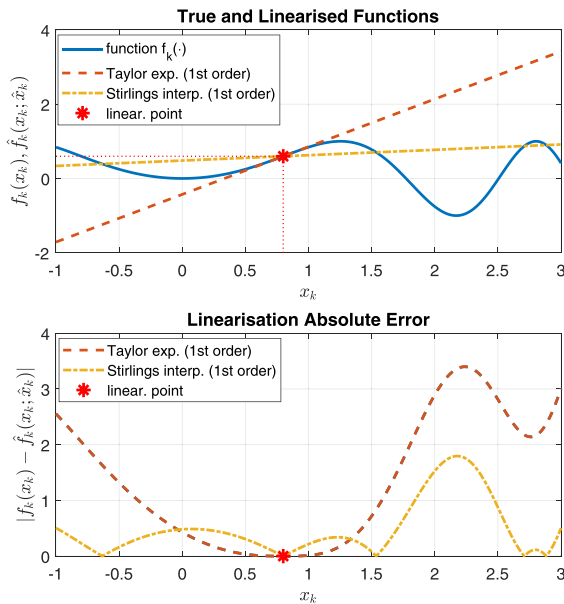


**Figure 2.** Illustration of derivative-based and derivative-free linearizations used in the LF design.

consistent results [22]–[26]. Roughly speaking, the LFs are expected to provide nearly optimal estimation performance for a mildly nonlinear model with an accurate initial condition.

## GLOBAL METHODS

As opposed to local methods, *global* methods provide accurate and consistent estimates in the form of conditional PDFs without any assumption of the conditional distribution family. Global methods are capable of estimating the state of a strongly nonlinear or non-Gaussian system, but usually at the cost of higher computational demands. Among these methods, the GSF [27], [28], the particle filter (PF) [2], [29], and the point-mass filter (PMF) [30], [31] have attracted considerable attention.

The GSF is based on the approximation of all conditional PDFs by weighted mixtures of Gaussian<sup>7</sup> densities [5], [32], [33] and an *analytical* solution to the BRRs. Then, the GSF can be imagined as a bank of simultaneously running LFs (e.g., EKFs or UKFs), which are weighted with respect to the available sequence of the measurements. As a consequence, the GSF is a *nonlinear* state estimator with respect to the measurement.

The PF and the PMF solve the integral BRRs (3), (4) *numerically*. The PF, developed in the nineties, is a representative of a statistical approach to solution of the BRRs. The main idea of the PF is to compute the conditional

PDF in the form of an empirical density, which consists of a finite set of random samples (or *particles*) and corresponding weights [29], [34], [35]. The central part of the statistical approach is the importance sampling technique, which uses an important function for drawing samples. The samples are then associated with the computed weights so that the samples and weights together correspond to the conditional PDF. On the other hand, the PMF, which was developed in the seventies, takes advantage of deterministic numerical integration rules. The fundamental step is an approximation of the continuous state-space by a grid of isolated points. Then, the conditional PDF is numerically computed at these grid points only [36], [37]. As a consequence, each point is associated with a computed conditional PDF value and a mass, where the value is assumed to be constant (thus, the name *point-mass*). Note that both the PF and PMF have been continually developed to increase the estimation quality and/or reduce computational complexity. Important among recent advancements are the particle flow, homotopy, and tensor-based methods [90]–[92], [99], [100].

Three typical approximations  $\hat{p}(x_k|z^k)$  of a scalar state variable conditional PDF  $p(x_k|z^k)$ , i.e., the mixture of Gaussians (for the GSF), the empirical PDF given by the samples (for the PF), and the PDF evaluated at a deterministically chosen grid of points (for the PMF), used in the GF design are visualized in Figure 3.

## STATE ESTIMATION METHODS: ADDITIONAL TOPICS

The state estimation overview, given in the previous section, provides a high-level description of the main research directions in the area. The research is, however, much wider and some of the topics, often stemming from application needs, are briefly mentioned below.

## BAYESIAN VERSUS OPTIMIZATION-BASED ESTIMATOR DESIGN

Besides the Bayesian approach to estimator design, there is also the optimization-based approach. Derivation of the optimization-based estimator starts with definition of the criterion to be minimized (e.g., minimal state estimate error) and possibly also with definition of the estimator structure (e.g., linear w.r.t. measurement). The resulting algorithm then provides estimates in the form of the conditional moments rather than the conditional PDF. The optimization-based estimators are represented, e.g., by the linear minimum mean square error (LMMSE) estimator<sup>8</sup> or the  $H_\infty$  filter [9], [23]. Although the Bayesian and optimization-based designs are principally different, they can

<sup>7</sup>A PDF can be approximated with a sum (or a mixture) of Gaussian PDFs with an arbitrary accuracy.

<sup>8</sup>The KF was originally developed as the LMMSE estimator [38].



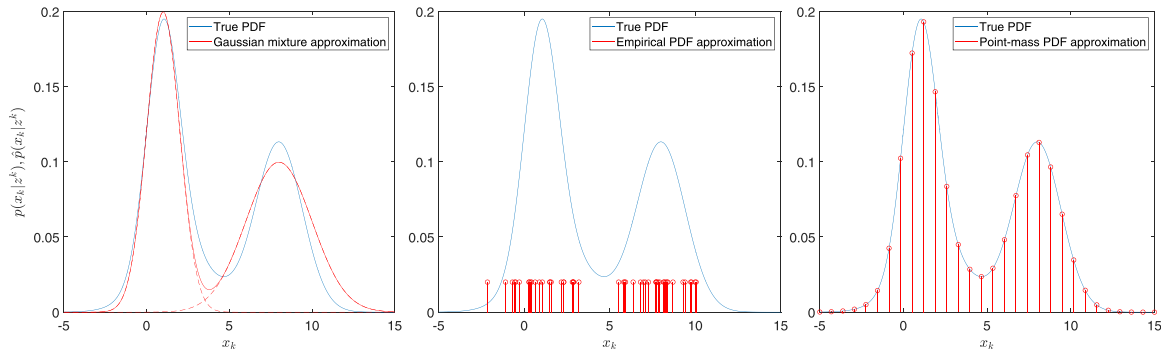

**Figure 3.**

Illustration of approximations used in the GF design; PDF approx. by Gaussian mixture (left plot), PDF approximation by empirical density (middle plot), PDF evaluated at grid points (right plot).

result in estimators which have the *same* algorithms but *different* assumptions.

### FILTERING, SMOOTHING, AND PREDICTION

State estimation can be divided into the three subtasks; *filtering*, where the conditional PDF  $p(\mathbf{x}_k | \mathbf{z}^k)$  is sought, *prediction*, where  $p(\mathbf{x}_{k+\ell} | \mathbf{z}^k)$  is sought, and *smoothing*, where  $p(\mathbf{x}_{k-\ell} | \mathbf{z}^k)$  is sought for  $\ell \geq 1$ . The previous section focused (explicitly) on the filtering and (implicitly) on the one-step prediction (because of the structure of the BRRs). However, all the filters mentioned have their multistep prediction and smoothing counterparts [2], [5], [8], [29], [37].

### CONTINUOUS VERSUS DISCRETE-TIME MODELS

In certain applications, navigation and tracking included, the available state-space model is *continuous-in-time*. In this case, the continuous model can be discretized and used for the abovementioned discrete estimator design or the purposely designed continuous-in-time estimators can be used. The filters mentioned have their counterparts for the continuous-in-time models [12], [23], [39], [40], [90], [92]. Moreover, for certain classes of continuous time nonlinear models, it is possible to find an exact state estimator. Examples from within this class of the exact estimators are the Beneš or Daum filters [95]–[97].

### GAUSSIAN VERSUS OTHER DENSITY SPECIFIC ESTIMATORS

The LFs are designed under the assumption of a Gaussian PDF for all random variables. The popularity of the Gaussian PDF arises from several reasons: 1) a Gaussian distribution appears quite often in nature, hence the statisticians use the term *normal* distribution; 2) a Gaussian PDF is fully characterized by the first two moments (thus, solution to the functional BRRs reduces to the recursive computation of the moments); 3) a Gaussian variable has

the largest entropy among all random variables of equal variance (i.e., the Gaussian assumption is the most conservative assumption in terms of entropy) [41]; 4) according to the central limit theorem, the sum of independent random variables approaches, under certain conditions, a Gaussian density [42]; and 5) algorithms for the Gaussian PDF can be relatively easily extended for a powerful Gaussian sum PDF. Despite all that, the Gaussian assumption may not be suitable for all applications and various (non-Gaussian) density specific estimators have been proposed. As an example, the following distributions have been considered in an estimator design.

- Student's  $t$ -distribution, which is a heavy tailed distribution suitable for modeling of uncertainties with frequent occurrence of outliers, was used in a design of the Student's  $t$ -filters [43]–[45].
- Rayleigh distribution, which is suitable for the formulation of the bearings-only tracking, was used in a design of the shifted Rayleigh filter [46].
- Circular, e.g., wrapped normal or von Mises, distributions, which are convenient for the description of angular quantities with bounded support, was used in a design of the circular filters [47], [48].
- The Gaussian scale mixture family of distributions, which is a family of distributions encompassing many of the above. Considering a Gaussian distribution whose means and variances are themselves random variables, one can account for a wide family of distributions depending on the distribution of those means and variances. This was exploited in [57]–[59] to design Gaussian filters that are able to deal with non-Gaussian distributions.

### CONSTRAINED ESTIMATION

The state estimation problem formulation typically assumes that the state is a real valued variable. However, it may

happen that the state domain is subject to certain constraints, e.g., estimated pressure cannot be negative, estimated vehicle position needs to be aligned with a road. Such constraints (belonging to *a priori* knowledge) cannot be incorporated in the state-space model to be straightforwardly used by the introduced state estimators. Therefore, various purposely designed approaches for constrained state estimation have been proposed [9], [49].

## MULTIPLE MODEL STATE ESTIMATION AND PARAMETER ESTIMATION

The nonlinear functions  $\mathbf{f}_k(\cdot)$  and  $\mathbf{h}_k(\cdot)$  of the model (1), (2) need not necessarily be smooth, but they can be viewed as a set of possibly simpler functions. As an example, consider (radar-based) tracking of aircraft, a highly manoeuvrable object. Aircraft dynamics can be described by a set of models, where each is suitable for the description of a different phase of flight (e.g., an almost constant velocity or acceleration model, a constant turn-rate model). During tracking, however, a suitable model can hardly be determined *a priori* as it is difficult to predict aircraft future manoeuvres. Therefore, the concept of the (interacting) multiple model (MM) has been developed [23]. The MM approach is based on the determination of a set of possible models of a system under different “working conditions.” For each model, then, a filter (typically an LF) is constructed and its likelihood w.r.t. available measurements is computed. The output of the MM filter can thus be either a weighted sum of all particular local estimates or the estimate with the highest likelihood. Note that the MM filter is algorithmically similar to the GSF. The MM approach has been significantly developed over recent years and MM-based state estimation approaches capable of tackling data association, clutter measurements, and estimating set variables have been proposed. Examples of these are the multiple hypothesis tracking filter and probability hypothesis density filter [101]–[104].

The MM approach is also suitable for tasks, where the state-space model contains parameter(s) that are unknown but can acquire a value from an *a priori* known set. Then, a set of filters is designed for each potential parameter value and is used in the MM filter [50]. Note that alternative approaches for concurrent estimation of the state and parameters are the joint and dual estimation approaches [51]. The former approach is based on extension of the state vector with the unknown parameters (resulting in the extended state-space model) and their simultaneous estimation by, typically, a nonlinear filter. The latter approach is based on a definition of two filters, which are regularly switched. The first one estimates the unknown states under the assumption of given parameters and the second one estimates the unknown parameters under the assumption of a given state.

## SOFTWARE TOOLS

An extensive number of state estimation algorithms have been proposed so far. It is, therefore, a challenging task to choose a suitable estimator for a given task or application. Fortunately, many of the estimators have been implemented and can be used for assessment (or prediction) of a filters’ performance. Most of the methods and toolboxes are designed for the MATLAB environment. The estimators are available in MATLAB proprietary toolboxes or in publicly available toolboxes. The latter includes, e.g., the *Nonlinear Estimation Framework* toolbox available at <http://nft.kky.zcu.cz/nef>, the *EKF/UKF Toolbox* available at <https://github.com/EEA-sensors/ekfukf>, or the *DynaEst Toolbox* available at <http://www.codeforge.com/article/41828>. A wide portfolio of routines for tracking is available in the *Tracking Component Library* available at <https://github.com/USNavalResearchLaboratory/TrackerComponentLibrary> [93]. Besides the toolboxes for the MATLAB, there are also early toolboxes in Python, a modern widely used programming language. An example is the International Society of Information Fusion (ISIF) StoneSoup initiative, which can be found at <https://stonesoup.readthedocs.io/en/latest/index.html>. Note that some books also come accompanied with sample implementations, e.g., [2], [4], [23].

## LITERATURE ON STATE ESTIMATION AND NAVIGATION

Because of the scope of this article, it was not possible to mention, discuss, and address all topics, details, and recent advancements in state estimation methods. Nevertheless, in the literature, there is an extensive number of comprehensive books and survey papers on state estimation and navigation system design, which offer an in-depth description of these areas. To name a few, the following references focused on estimation theory [1], [2], [5], [9], [12], [16], [29], [34], [52] and navigation system design [3], [4], [23], [60], [105].

## ESTIMATION IN NAVIGATION SYSTEMS

The origin of state estimation methods is closely associated with the development of navigation and tracking systems. Indeed, any modern navigation system uses a state estimation algorithm for optimal processing of data from a variety of sensors. In this section, recent developments and examples of application of state estimation methods are provided with the stress on the area of expertise of the AESS NSP members. Besides recent navigation applications, this section also discusses their expected level of nonlinearity/non-Gaussianity and error sources of the sensors and maps typically used in the navigation system. Knowledge of the considered task nonlinearity/non-Gaussianity and correct treatment of the sensor (or map) error sources is essential for the selection of the appropriate

state estimator and achievement of a high and consistent navigation performance.

### EXTENDED KALMAN FILTER IN ATTITUDE AND HEADING REFERENCE SYSTEM

An attitude and heading reference system (AHRS) is an inertial-measurement-based navigation system providing an estimate of the vehicle attitude (i.e., deviation of the vehicle orientation from its tangential plane) and heading (i.e., difference between vehicle heading and geographic north) [53]. Considering pure inertial AHRS and lower cost microelectromechanical system (MEMS) inertial sensors without a capability of gyro-compassing, the vehicle attitude and heading are computed from two pairs of noncollinear vectors. Typically, the vectors of gravity field and magnetic field are considered. Then, the first pair consists of two vectors of gravity field, where one vector is the gravity vector in the body frame measured by the accelerometer and the other is the expected gravity field vector in the navigation frame computed on the basis of a model (e.g., the Earth Gravitational Model EGM96). The second pair consists of the magnetic field vectors, where the magnetometer's measured vector is in the body frame and the other is the expected magnetic field vector in the navigation frame computed on the basis of a model (e.g., the International Geomagnetic Reference Field model IGRF-13).

In [53], the EKF-based pure inertial AHRS was designed. The AHRS was developed with the stress on the adaptive elimination of nongravitational vehicle acceleration, which can be considered as the main error source. The proposed AHRS thus provides *accurate* and *consistent* estimates even in highly dynamic trajectories. Note that the AHRS performance was illustrated using synthetic and real data following the RTCA DO-334 Minimum Operational Performance Standard requirements. The AHRS is further discussed and its performance is illustrated in [54].

In Figure 4, an AHRS system is qualitatively compared in terms of the degree of nonlinearity and non-Gaussianity of the corresponding technical challenges. Particularly, the abscissa axis of the diagram represents the linearity/nonlinearity of the problem, and the ordinate axis shows the degree of non-Gaussianity. For the AHRS, the majority of the complications involve nonlinearities due to unavailable magnetometer measurements or growing heading information uncertainty.

### PMF IN TERRAIN-AIDED NAVIGATION (TAN) SYSTEM

A TAN system is primarily designed for environments, where the coverage of radio navigation systems (e.g., GNSS or distance measuring equipment) is not expected to be

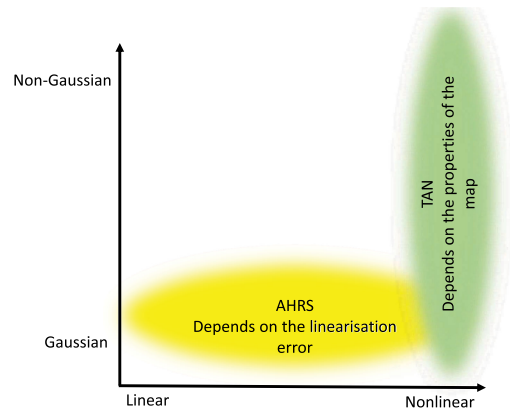


**Figure 4.** Categorization of typical problems in AHRS and TAN systems.

sufficient or the transmission of the radio navigation systems can be interfered with (e.g., by jamming or spoofing) [55]. Unlike radio navigation systems, the TAN systems determine the position of a land, air, or water vehicle on the basis of on-board sensor measurements and a map of the terrain covering the vicinity of the vehicle. As a consequence, TAN systems do not rely on any information broadcast to the vehicle from distant systems and thus they are much more resistant to intentional or unwitting interference.

TAN systems are, in principle, highly nonlinear. As such, global (and computationally demanding) estimation algorithms are used for measurement and map processing. In [55] and [56], a novel *computationally efficient* version of the PMF, namely, the Rao–Blackwellised PMF (RBPMF), was proposed, which provides highly accurate and consistent estimates for a class of conditionally linear models, typically, appearing in the area of navigation. The developed RBPMF was used in a TAN system and evaluated using a set of synthetic and real data.

As can be seen in Figure 4, a TAN system is a highly nonlinear estimation task, mainly due to the utilization of the terrain map (terrain, as modeled in the state-space model, can be viewed as a complex nonlinear function). The degree of the non-Gaussianity depends on the data source used for the map design (e.g., from satellite, aircraft, or LiDAR based mapping).

### GLOBAL NAVIGATION SATELLITE SYSTEMS

When available, satellite-based navigation is arguably *the* solution for positioning, navigation, and timing (PNT) [62], [63], [73]. The overarching technological name is GNSSs, which encompasses GPS, GALILEO, GLONASS, Beidou, and other regional and augmentation systems [60], [89]. All these systems share the same principle: a constellation of satellites transmit spread-spectrum signals that the receiver uses to estimate its (pseudo-)distances to those satellites, which are then used in solving a geometrical problem to

compute position and timing with an accuracy that ranges from a couple of meters to centimeters depending on the type of signals, frequencies, and method (code/carrier) used in such processing. Remarkably, a GNSS receiver leverages state estimation in several of its building blocks, which are briefly discussed hereafter.

Whereas acquisition of GNSS signals is typically considered as a detection (or classification) problem, the fine estimation of the time-varying delay/Doppler parameters of the signals is performed by the so-called tracking loops. Those delay and phase lock loops (DLL and PLL, respectively), as well as its different variants, can be considered instances of a larger state estimation framework where the gain is fixed (selected through the choice of a loop bandwidth). For instance, Vilá-Valls[64] provided a tutorial review of KF-based carrier tracking techniques for GNSS receivers, highlighting their relationship with legacy PLL schemes. The use of state estimation to substitute standard tracking loops was seen to be a promising tool in many challenging scenarios such as in mitigating the effects of ionospheric scintillation [65], [66], mitigating multipath propagation [67], enabling resilient noncoherent tracking of data-only channels [68], attenuating the effects of interference [70], coping with high, time-varying dynamics [71], or in designing robust real-time kinematic (RTK) solutions in harsh propagation conditions [72], to name a few examples.

In the context of position, velocity, and time (PVT) estimation, whereas estimation of  $\mathbf{x}_k$  (i.e., containing the PVT variables) can be carried out on an epoch-per-epoch basis if signals from four or more GNSS satellites are observed, the use of state estimation techniques (mostly KFs) typically improves the overall performance due to two facts [87]. First, the use of  $\mathbf{f}_k(\cdot)$  from (1) to model the receiver antenna motion constrains the degrees of freedom of the unknown variable. In the case where an IMU is available, the filter state  $\mathbf{x}_k$  becomes the error of the inertial strapdown computation and  $\mathbf{f}_k(\cdot)$  becomes a system model for those error states, thereby even further limiting the degrees of freedom that need to be solved by the GNSS observations (mainly IMU alignment and biases) [4]. Second, the state vector can be tailored to include GNSS-specific artefacts, like carrier phase ambiguities. The state estimation technique is additionally used to fuse information from both code-phase (a.k.a. pseudorange) and carrier-phase observables in a variety of ways. The resulting carrier-phase positioning techniques like carrier/Doppler-smoothing, RTK or precise-point-positioning are then typically implemented by means of (more or less sophisticated) versions of KF-like algorithms [85], [86].

GNSS, like many radio-navigation systems, provides measurements through a correlation process [88] and  $\mathbf{h}_k(\cdot)$  in (2) ideally captures all aspects of this. In open-sky conditions, DLL or PLL discriminators (plus the loop filters) provide good approximations via linearization of the

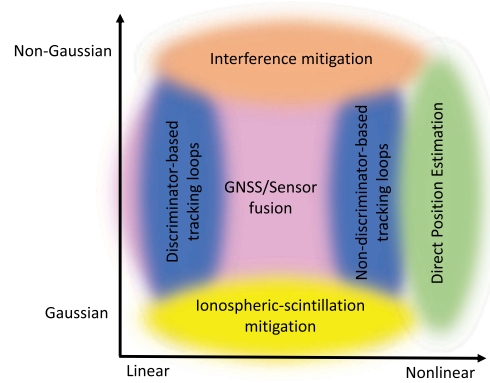


**Figure 5.**

Categorization of typical signal processing problems in GNSS receiver design.

correlation functions and a linear  $\mathbf{h}_k(\cdot)$  well approximates the real circumstances. However, in adverse signal conditions such as multipath, urban, or indoor scenarios, the conventionally used discriminators do not provide accurate approximations, and as a consequence the resulting state estimates including the covariance are far from reflecting the real distribution of the user's position. To circumvent these issues, Bayesian direct position estimation (BDPE) uses the correlation values at several time-delay/Doppler-shifts directly as measurements and  $\mathbf{h}_k(\cdot)$  is given by the signal's correlation function and thus becomes nonlinear [79]. To solve the resulting nonlinear state estimation both Gaussian derivative-free filtering [80] and PF [83] methods were considered in the literature. The latter showed, in real-world adverse signal conditions, that non-Gaussian (even multimodal) PDFs for the user position may occur, thus the PF implementation provides more realistic PDF estimates at the expenses of an increased computational cost. BDPE (and DPE) was also shown to provide higher sensitivity and resilience [81] since it increases the effective signal-to-noise ratio by combining the signals from different satellites as opposed to legacy receivers [82]. However, BDPE is orders of magnitude more computationally demanding than DLL/PLL tracking plus KF-based PVT solvers. It is also more difficult to tune and requires handling of satellite ephemeris or atmospheric errors as nuisance parameters [84]. Furthermore, modeling  $\mathbf{h}_k(\cdot)$  via the correlation function is still an approximation and a more complete formulation requires stochastic modeling of propagation channel parameters or inclusion of multipath reflection parameters in the state vector  $\mathbf{x}_k$ .

A qualitative diagram of challenging GNSS areas can be observed in Figure 5, similarly to that in Figure 4 for AHRS and TAN systems. In this case, we highlight that jamming interference may cause saturation of the analog-to-digital (ADC) converters, bringing non-Gaussianity to the measurements. Implementing tracking using a discriminator-based



approach allows for linear modeling of the resulting observations, but might yield to compromising the Gaussian assumption. If a discriminator is not considered, the filtering method needs to account for nonlinearities in the model. Ionospheric scintillation is typically modeled through Gaussian linear/nonlinear dynamics. Multipath modeling is either nonlinear Gaussian if done at the sampled signal level, or nonlinear/non-Gaussian if done at the observable level due to the biases it produces on range estimates. As mentioned earlier, DPE presents a challenging nonlinear problem that, in turn, can be Gaussian or non-Gaussian depending on the multipath conditions and other interfering sources. Fusion of GNSS data and other sensors gives rise to a multitude of architectures that, basically, can populate the four main quadrants in Figure 5.

## SPACE VEHICLE NAVIGATION

Accurate navigation of space vehicles is crucial for the success of space missions. Precise position and velocity information is essential for the insertion of a spacecraft into an orbit, in-orbit station keeping, guidance, and manoeuvring of satellites. The navigation system plays an even more vital role in planetary reentry missions. Precise orbit determination (POD), i.e., position estimation with highest possible accuracy is essential for synthetic aperture radar, altimetry, GNSS radio occultation, and gravimetry missions. Various state estimation techniques are used to estimate position and velocity of a space vehicle from various types of observations, for example, dead-reckoning, range, range rate, pointing angle, angular measurements to known celestial objects.

This task is nonlinear, so the EKF is a widely used estimation algorithm for the space vehicle navigation. An example of EKF-based low Earth orbit (LEO) satellite navigation using GNSS code and carrier-phase observations can be found in [74]. Navigation of a spacecraft in the lunar transfer trajectory using ground-based range, range-rate, and angular observations can also be performed using a sequential state estimator like the EKF [75]. It should be noted that the EKF provides a sub-optimal estimation solution due to the linearization in the mean and covariance matrix propagation equations. For this reason, the position solution of the EKF can be degraded for reentry and launch vehicle navigation problems, where the dynamics of the space vehicles are highly nonlinear [16], [76]. The UKF can be used in these state estimation problems to obtain better navigation performance. However, the UKF is more computationally expensive due to multiple sample state vector propagations at each measurement interval and hence it is often difficult to implement for real-time applications. The single propagation unscented Kalman filter and the

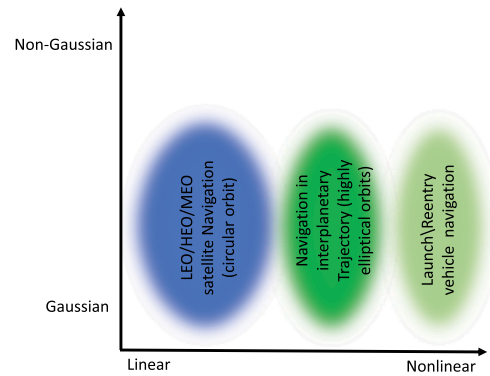


**Figure 6.**

Categorization of typical problems in Space Vehicle Navigation systems.

extrapolated single propagation unscented Kalman filter have been developed [76] to address this issue. These estimators can reduce the computation time of the UKF by up to 90%[77]. In other words, the accuracy of the UKF can be delivered with the computational complexity of the EKF. Using a similar approach, a computationally efficient PF has been proposed as well which can be used for real-time navigation [78]. The accuracy of the PF can be delivered using this algorithm with around 90% reduction in computation time.

It should be noted that in the state estimation problem for space vehicle navigation, the dynamics of the space vehicle can be mildly nonlinear to highly nonlinear, depending on the type of vehicle [105]. The process noise and measurement noise are considered zero-mean Gaussian in most cases [106]–[110]. However, the process noise for the space vehicle motion model arises from the unaccounted perturbation forces, which is non-Gaussian in nature [111]. Considering the process noise as Gaussian is an approximation and results in a relatively less accurate navigation solution. For high precision applications like POD, all the perturbation forces need to be modeled carefully and then the process noise can be considered as Gaussian [112]. The qualitative diagram is shown in Figure 6 in this case.

## TREATMENT OF ERROR SOURCES

Navigation systems use a wide range of sensors, which provide measurements  $\mathbf{z}_k$  or data  $\mathbf{u}_k$  used for the state measurement update [filtering step (3)] or the state time update [prediction step (4)], respectively. Realistic modeling of sensors for the navigation filter algorithm design is, therefore, essential to achieve high navigational performance. However, at the same time, it is a complex task requiring a deep knowledge of underlying physical principles and mathematical background that can often be fulfilled only approximately. To at least partially capture this

Table 1.

Character of Various Navigation Sensor (Including the Map) Error Sources				
		Linearity of deterministic part of error model	PDF of stochastic part of error model	Temporal/spatial correlation of error
GNSS satellite	nominal satellite orbit errors	linearity given due to large distance satellite-user	approximately Gaussian	highly correlated in time
	satellite orbit anomalies (determination/upload gross errors, unflagged maneuvers, eclipsing, ...)	–	–	rarely occurring gross errors
	nominal satellite clock errors	linear	approximately Gaussian	highly correlated in time
	satellite clock anomalies (clock drifts, jumps,...)	–	–	rarely occurring gross errors
	satellite payload failures resulting in signal waveforms anomalies	nonlinear	–	nearly constant in time
	satellite hardware delays	linear	–	highly correlated in time (dependent on payload temperature)
GNSS signal propagation	tropospheric modelling errors	linear	approximately Gaussian	correlated in time and space (weather dependent)
	ionospheric modelling errors (single frequency user)	linear	approximately Gaussian	correlated in time and space (space weather dependent)
	residual ionospheric errors after compensation for dual (or more) frequency user	–	non-Gaussian	correlated in time (space weather dependent, scintillations)
	multipath impact at user side	nonlinear	non-Gaussian	correlated, depending of geometry change
	jamming at user side	–	zero-mean Gaussian for low power, non-Gaussian for high-power	white
	spoofing at user side	–	–	gross ranging errors
GNSS receiver	thermal noise at user receiver (antenna, frontend)	–	zero-mean Gaussian	white
	nominal tracking loop noise (thermal, transient, oscillator jitter)	–	approximately Gaussian	correlated pending user dynamics, oscillator type and tracking settings
	erratic tracking loop response in harsh signal conditions including cycle-slips	unknown	non-Gaussian	approximately white
	receiver hardware delays	linear	–	correlated in time (dependent on frontend/antenna temperature)
	unmodelled antenna phase center variations at user side	linear	–	highly correlated in time depending on direction of arrival to user antenna
Inertial sensors	bias (turn-on, run-to-run, constant)	linear	Gaussian	time-correlated (time constant depends on the IMU grade, magnitude depends on the quality of IMU laboratory calibration)

Table 1.

(Continued)				
		Linearity of deterministic part of error model	PDF of stochastic part of error model	Temporal/spatial correlation of error
	misalignment error (scale-factor, cross-coupling)	linear	–	constant (magnitude depends on the quality of IMU factory calibration)
	random noise (residual electrical noise, quantization, vibration)	–	Gaussian	white
	scale factor nonlinearity	nonlinear	–	constant
Magnetometer	additive magnetic field produced by e.g., by permanent magnet, electrical equipment (hard-iron bias)	linear	Gaussian/non-Gaussian based on operation conditions	time-correlated
	distortion of magnetic field by e.g., surrounding iron (soft-iron bias)	nonlinear	Gaussian/non-Gaussian	time-correlated
	misalignment error (analogous to inertial sensors)	linear	–	constant
	random noise	linear	Gaussian	white
Altimeter	weather variation	linear	Gaussian	time-correlated
Map (as an aiding source or its part)	terrain (e.g., SRTM), magnetic field (e.g., IGRF-13, WMM), gravity field (e.g., EGM96), ionosphere (e.g., Klobuchar, NeQuick)	linear	Gaussian/non-Gaussian	typically spatially correlated, properties depends on the map/model design technology and source data

complexity Table 1 is provided, which gives an overview for error sources of the sensors typically considered in the four mentioned navigation systems.

In the case of GNSS, the impact of the error source on range measurements (code or carrier observables) is discussed and it should be noted that the impact might have a different characterization on raw signals or correlation values. The GNSS satellite is considered in this context as a sensor whose various error modes result in biased range measurements. Gross errors can be handled via multiple hypothesis filters. Errors with a deterministic impact on the range are denoted with the symbol “–” in the “PDF” column. Most noteworthy is the correct handling of temporal or spatial correlations. Modeling of atmospheric errors as range biases within the navigation filter is often essential for utmost accuracy, but requires a simplified treatment of atmospheric physics. Errors related to multiple propagation paths and from the signal processing within the GNSS receivers can be considered linear and Gaussian for nominal open-sky conditions but become highly nonlinear and non-Gaussian in adverse signal conditions.

The INS processes the inertial measurement data (and also measurements of other nonradiating sensors such as the magnetometer or the barometric altimeter) *nonlinearly*, because the dynamic model of the time evolution of the navigation parameters is nonlinear.<sup>9</sup> However, certain errors (such as biases) are modeled linearly (e.g., by a Gauss–Markov process) and then just subtracted from the measurements. The models are typically linear although the error’s physical cause can be a nonlinear function of the surrounding environmental effects. On the other hand, for example, misalignment and scaling of a tri-axis sensor can be dealt with by simply multiplying the true quantity by typically a  $3 \times 3$  matrix, which is a linear operation from the physical perspective. Another issue is that certain parameters of the sensors are calibrated offline potentially by a nonlinear optimization and then these parameters are used in the design of a linear error model [113]–[115]. Because of the multiple possible views on the sensor error properties and their respective models, the table below

<sup>9</sup>The nonlinear model can be, for the purpose of the state estimation, linearized.

gives an overview of the dominant errors affecting the sensor readings with the emphasis on the properties of the error models used in the navigation filter. It should be also noted that the error properties are closely tied with the sensor grade and in the table higher sensor grades, as used in navigation systems, are considered.

An insubstitutable component of any navigation system is an explicit or implicit model (or map) of an environmental feature. Of the former type, the terrain map<sup>10</sup> used as an aiding source of the TAN system is worth mentioning here. The latter type includes for example models of the gravity field<sup>11</sup> (e.g., the EGM96 [4]), magnetic field (e.g., the IGRF-13, the world magnetic model (WMM) [4]), or of the ionosphere (e.g., Klobuchar, NeQuick [4]). Quality of such maps and models determines, to a certain extent, the overall performance of the navigation system and thus their errors should be also carefully treated. The map error is, therefore, included in the table for the sake of completeness.

Finally, it is worth noting that the correct modeling of the navigated vehicle dynamics within the state equation and the function  $\mathbf{f}_k(\cdot)$  is at least equally important as the sensor modeling. However, due to the near endless variety of vehicle motion patterns, it becomes nearly impossible to present a concise overview in this table. Details and discussion on the models used in the navigation or tracking can be found, for instance, in [3], [4], and [23] and references therein.

## CONCLUDING REMARKS

This article dealt with state estimation of the nonlinear stochastic dynamic discrete-in-time systems. In particular, stress was laid on a high-level overview of the state-of-the-art Bayesian state estimation methods and description of their applications in the area of navigation and tracking system design. The field is steadily growing with more efficient, generic, and robust filtering methodologies, research mostly ignited by the plethora of applications leveraging state estimation developments.

## ACKNOWLEDGMENTS

J. Duník, A. G. Dempster, T. Pany, and P. Closas are members of the IEEE Aerospace and Electronic Systems

Navigation Systems Panel. The work of J. Duník was partially supported by the Czech Science Foundation under Grant GA 20-06054. The work of J. P. Closas was partially supported by the National Science Foundation under Awards CNS-1815349 and ECCS-1845833.

## REFERENCES

- [1] B. P. Gibbs, *Advanced Kalman Filtering, Least-Squares and Modelling*. Hoboken, NJ, USA: Wiley, 2011.
- [2] S. Särkkä, *Bayesian Filtering and Smoothing*. Cambridge, U.K.: Cambridge Univ. Press, 2013.
- [3] R. M. Rogers, *Applied Mathematics in Integrated Navigation Systems*, 2nd ed. Reston, VA, USA: AIAA, 2003.
- [4] P. D. Groves, *Principles of GNSS, Inertial, and Multisensor Integrated Navigation Systems*. Norwood, MA, USA: Artech House, 2008.
- [5] B. D. O. Anderson and J. B. Moore, *Optimal Filtering*. Englewood Cliffs, NJ, USA: Prentice-Hall, 1979.
- [6] H. W. Sorenson, "On the development of practical nonlinear filters," *Inf. Sci.*, vol. 7, pp. 230–270, 1974.
- [7] I. Arasaratnam and S. Haykin, "Cubature Kalman filters," *IEEE Trans. Autom. Control*, vol. 54, no. 6, pp. 1254–1269, Jun. 2009.
- [8] M. Šimandl and J. Duník, "Derivative-free estimation methods: New results and performance analysis," *Automatica*, vol. 45, no. 7, pp. 1749–1757, 2009.
- [9] D. Simon, *Optimal State Estimation: Kalman, H Infinity, and Nonlinear Approaches*. Hoboken, NJ, USA: Wiley-Interscience, 2006.
- [10] R. Henriksen, "The truncated second-order nonlinear filter revised," *IEEE Trans. Autom. Control*, vol. 27, no. 1, pp. 247–251, Feb. 1982.
- [11] J. Vilà-Valls, P. Closas, and A. García-Fernández, "Uncertainty exchange through multiple quadrature Kalman filtering," *IEEE Signal Process. Lett.*, vol. 23, no. 12, pp. 1825–1829, Dec. 2016.
- [12] A. H. Jazwinski, *Stochastic Processes and Filtering Theory*. New York, NY, USA: Academic, 1970.
- [13] L. Meier, "The third order extended Kalman filter," in *Proc. 2nd Symp. Nonlinear Estimation Theory Appl.*, San Diego, CA, USA, 1971, pp. 997–1009.
- [14] T. S. Schei, "A finite-difference method for linearization in nonlinear estimation algorithms," *Automatica*, vol. 33, no. 11, pp. 2053–2058, 1997.
- [15] M. Nørgaard, N. K. Poulsen, and O. Ravn, "New developments in state estimation for nonlinear systems," *Automatica*, vol. 36, no. 11, pp. 1627–1638, 2000.
- [16] S. J. Julier and J. K. Uhlmann, "Unscented filtering and nonlinear estimation," *IEEE Proc.*, vol. 92, no. 3, pp. 401–421, Mar. 2004.
- [17] K. Ito and K. Xiong, "Gaussian filters for nonlinear filtering problems," *IEEE Trans. Autom. Control*, vol. 45, no. 5, pp. 910–927, May 2000.

<sup>10</sup>As an example of publicly available source, the Shuttle Radar Topography Mission (SRTM) maps, available at <https://www2.jpl.nasa.gov/srtm/>, can be mentioned.

<sup>11</sup>The mentioned models such as the EGM96 are low resolution models. For precise navigation maps of magnetic and gravity fields anomalies may be required. The gravity anomaly models are available, e.g., at <http://icgem.gfz-potsdam.de/home>.



- [18] Y. Wu, D. Hu, M. Wu, and X. Hu, "A numerical-integration perspective on Gaussian filters," *IEEE Trans. Signal Process.*, vol. 54, no. 8, pp. 2910–2921, Aug. 2006.
- [19] B. Jia, M. Xin, and Y. Cheng, "Sparse Gauss–Hermite quadrature filter with application to spacecraft attitude estimation," *J. Guid., Control, Dyn.*, vol. 34, no. 2, pp. 367–379, 2011.
- [20] J. Duník, O. Straka, M. Šimandl, and E. Blasch, "Random-point-based filters: Analysis and comparison in target tracking," *IEEE Trans. Aerosp. Electron. Syst.*, vol. 51, no. 2, pp. 303–308, Apr. 2015.
- [21] T. Lefebvre, H. Bruyninckx, and J. De Schuller, "Comment on 'A new method for the nonlinear transformation of means and covariances in filters and estimators,'" *IEEE Trans. Autom. Control*, vol. 47, no. 8, pp. 1406–1409, Aug. 2002.
- [22] K. Reif, S. Günther, E. Yaz, and R. Unbehauen, "Stochastic stability of the discrete-time extended Kalman filter," *IEEE Trans. Autom. Control*, vol. 44, no. 4, pp. 714–728, Apr. 1999.
- [23] Y. Bar-Shalom, X. R. Li, and T. Kirubarajan, *Estimation With Applications to Tracking and Navigation: Theory Algorithms and Software*. Hoboken, NJ, USA: Wiley, 2001.
- [24] X. R. Li, "Measure of nonlinearity for stochastic systems," in *Proc. 15th Int. Conf. Inf. Fusion*, Singapore, 2012.
- [25] J. Duník, O. Straka, and A. F. García-Fernández, "Performance evaluation of nonlinearity and non-Gaussianity measures in state estimation," in *Proc. 20th Int. Conf. Inf. Fusion*, Xian, China, 2017, pp. 1073–1080.
- [26] J. Duník and O. Straka, "State estimate consistency monitoring in Gaussian filtering framework," *Signal Process.*, vol. 148, pp. 145–156, 2018.
- [27] H. W. Sorenson and D. L. Alspach, "Recursive Bayesian estimation using Gaussian sums," *Automatica*, vol. 7, pp. 465–479, 1971.
- [28] M. Šimandl and J. Královec, "Filtering, prediction and smoothing with Gaussian sum representation," in *Proc. 12th Symp. Syst. Identification*, 2000, pp. 1157–1162.
- [29] A. Doucet, N. De Freitas, and N. Gordon, Eds., *Sequential Monte Carlo Methods in Practice*. New York, NY, USA: Springer, 2001.
- [30] M. Šimandl, J. Královec, and T. Söderström, "Anticipative grid design in point-mass approach to nonlinear state estimation," *IEEE Trans. Autom. Control*, vol. 47, no. 4, pp. 699–702, Apr. 2002.
- [31] J. Královec and M. Šimandl, "Filtering, prediction and smoothing with point-mass approach," in *IFAC Proc. Vol.*, vol. 37, pp. 375–380, 2004.
- [32] M. Šimandl and J. Duník, "Sigma point Gaussian sum filter design using square root unscented filters," *IFAC Proc. Vol.*, vol. 38, pp. 1000–1005, 2005.
- [33] X. Luo, I. M. Moroz, and I. Horeit, "Scaled unscented transform Gaussian sum filter: Theory and application," *Physica D*, vol. 239, no. 10, pp. 684–701, 2010.
- [34] S. Arulampalam, S. Maskell, N. Gordon, and T. Clapp, "A tutorial on particle filters for on-line non-linear/non-Gaussian Bayesian tracking," *IEEE Trans. Signal Process.*, vol. 50, no. 2, pp. 174–188, Feb. 2002.
- [35] F. Gustafsson, "Particle filter theory and practice with positioning applications," *IEEE Aerosp. Electron. Syst. Mag.*, vol. 25, no. 7, pp. 53–82, Jul. 2010.
- [36] R. S. Bucy and K. D. Senne, "Digital synthesis of non-linear filters," *Automatica*, vol. 7, pp. 287–298, 1971.
- [37] M. Šimandl, J. Královec, and T. Söderström, "Advanced point-mass method for nonlinear state estimation," *Automatica*, vol. 42, no. 7, pp. 1133–1145, 2006.
- [38] R. E. Kalman, "A new approach to linear filtering and prediction problems," *Trans. ASME—J. Basic Eng.*, vol. 82, pp. 35–45, 1960.
- [39] C. Kalender and A. Schöttl, "Sparse grid-based nonlinear filtering," *IEEE Trans. Aerosp. Electron. Syst.*, vol. 49, no. 4, pp. 2386–2396, Oct. 2013.
- [40] O. Straka, J. Duník, and M. Šimandl, "Design of discrete second order filters for continuous-discrete models," in *Proc. 18th Int. Conf. Inf. Fusion*, Washington, DC, USA, 2015, pp. 1825–1832.
- [41] A. Hyvärinen, and E. Oja, "Independent component analysis: Algorithms and applications," *Neural Netw.*, vol. 13, pp. 411–430, 2000.
- [42] A. Papoulis and S. U. Pillai, *Probability, Random Variables and Stochastic Processes*. 4th ed. New York, NY, USA: McGraw Hill, 2002.
- [43] M. Roth, E. Özkan, and F. Gustafsson, "A Student's t-filter for heavy tailed process and measurement noise," in *Proc. IEEE Int. Conf. Acoust., Speech Signal Process.*, Vancouver, Canada, May 2013, pp. 5770–5774.
- [44] F. Tronarp, R. Hostettler, and S. Särkkä, "Sigma-point filtering for nonlinear systems with non-additive heavy-tailed noise," in *Proc. 19th Int. Conf. Inf. Fusion*, Heidelberg, Germany, 2016.
- [45] O. Straka and J. Duník, "Stochastic integration Student's t-filter," in *Proc. 20th Int. Conf. Inf. Fusion*, Xi'an, China, 2017.
- [46] J. M. C. Clark, R. B. Vinter, and M. M. Yaqoob, "Shifted Rayleigh filter: A new algorithm for bearings-only tracking," *IEEE Trans. Aerosp. Electron. Syst.*, vol. 43, no. 4, pp. 1373–1384, Oct. 2007.
- [47] G. Kurz, I. Gilitschenski, and U. D. Hanebeck, "Recursive nonlinear filtering for angular data based on circular distributions," in *Proc. Amer. Control Conf.*, Washington, DC, USA, 2013, pp. 5439–5445.
- [48] G. Kurz, I. Gilitschenski, and U. D. Hanebeck, "Recursive Bayesian filtering in circular state spaces," *IEEE Aerosp. Electron. Syst. Mag.*, vol. 31, no. 3, pp. 70–87, Mar. 2016.
- [49] O. Straka, J. Duník, and M. Šimandl, "Truncation nonlinear filters for state estimation with nonlinear inequality constraints," *Automatica*, vol. 48, no. 2, pp. 273–286, 2012.

- [50] D. G. Lainiotis, "Optimal adaptive estimation: Structure and parameters adaptation," *IEEE Trans. Autom. Control*, vol. 16, no. 2, pp. 160–170, Apr. 1971.
- [51] E. A. Wan, R. van der Merwe, and A. T. Nelson, "Dual estimation and the unscented transformation," in *Proc. NIPS Int. Conf. Neural Inf. Process. Syst.*, Denver, CO, USA, Nov. 1999, pp. 666–672.
- [52] M. Roth, G. Hendeby, F. Gustafsson, "Nonlinear Kalman filters explained: A tutorial on moment computations and sigma point methods," *J. Adv. Inf. Fusion*, vol. 11, no. 1, pp. 47–70, 2016.
- [53] P. Malinák, M. Soták, Z. Kaňa, R. Baránek, and J. Duník, "Pure-inertial AHRS with adaptive elimination of non-gravitational vehicle acceleration," in *Proc. IEEE/ION Position Location Navigation Symp.*, Monterey, CA, USA, May 2018, pp. 696–707.
- [54] Z. Kaňa et al., "GPAHRS—Navigation enabler for more autonomous aircraft," in *Proc. Aerosp. Eur. Conf.*, Bordeaux, France, Feb. 2020.
- [55] J. Duník, M. Soták, M. Veselý, O. Straka, and W. J. Hawkinson, "Design of Rao–Blackwellised point-mass filter with application in terrain aided navigation," *IEEE Trans. Aerosp. Electron. Syst.*, vol. 55, no. 1, pp. 251–272, Feb. 2019.
- [56] J. Duník, M. Soták, M. Veselý, and W. J. Hawkinson, "Apparatus and method for data-based referenced navigation," Patent Application US 15/373 999 0912, 2016.
- [57] J. Vilà-Valls, P. Closas, C. Fernández-Prades, and J. A. Fernández-Rubio, "Nonlinear Bayesian filtering in the Gaussian scale mixture context," in *Proc. 20th Eur. Signal Process. Conf.*, Bucharest, Romania, Aug. 2020, pp. 529–533.
- [58] P. Closas and J. Vilà-Valls, "NLOS mitigation in TOA-based indoor localization by nonlinear filtering under skew t-distributed measurement noise," in *Proc. IEEE Statist. Signal Process. Workshop*, Palma de Mallorca, Spain, Jun. 2016, pp. 1–5.
- [59] J. Vilà-Valls and P. Closas, "NLOS mitigation in indoor localization by marginalized Monte Carlo Gaussian smoothing," *EURASIP J. Advances Signal Process.*, vol. 2017, 2017, Art. no. 62.
- [60] E. Kaplan, and C. Hegarty, Eds., *Understanding GPS/GNSS: Principles and Applications*. Norwood, MA, USA: Artech House, 2017.
- [61] K. Borre, D. M. Akos, N. Bertelsen, P. Rinder, and S. H. Jensen, *A Software-Defined GPS and Galileo Receiver: A Single-Frequency Approach*. Berlin, Germany: Springer, 2007.
- [62] M. G. Amin, P. Closas, A. Broumandan, and J. Vola-kis, "Vulnerabilities, threats, and authentication in satellite-based navigation systems [scanning the issue]," *Proc. IEEE*, vol. 104, no. 6, pp. 1169–1173, Jun. 2016.
- [63] P. Closas, M. Luise, J. Àvila-Rodríguez, C. Hegarty, and J. Lee, "Advances in signal processing for GNSSs [From the Guest Editors]," *IEEE Signal Process. Mag.*, vol. 34, no. 5, pp. 12–15, Sep. 2017.
- [64] J. Vilà-Valls, P. Closas, M. Navarro, and C. Fernández-Prades, "Are PLLs dead? A tutorial on Kalman filter-based techniques for digital carrier synchronization," *IEEE Aerosp. Electron. Syst. Mag.*, vol. 32, no. 7, pp. 28–45, Jul. 2017.
- [65] J. Vilà-Valls, P. Closas, and J. T. Curran, "Multi-frequency GNSS robust carrier tracking for ionospheric scintillation mitigation," *J. Space Weather Space Climate*, vol. 7, 2017, Art. no. A26.
- [66] J. Vilà-Valls, P. Closas, C. Fernández-Prades, and J. T. Curran, "On the mitigation of ionospheric scintillation in advanced GNSS receivers," *IEEE Trans. Aerosp. Electron. Syst.*, vol. 54, no. 4, pp. 1692–1708, Aug. 2018.
- [67] P. Closas, C. Fernández-Prades, and J. A. Fernández-Rubio, "A Bayesian approach to multipath mitigation in GNSS receivers," *IEEE J. Sel. Topics Signal Process.*, vol. 3, no. 4, pp. 695–706, Aug. 2009.
- [68] M. Susi and D. Borio, "Galileo E6-B tracking with non-coherent integration and Kalman filtering," in *Proc. 32nd Int. Tech. Meeting Satellite Division Inst. Navigation*, Miami, FL, USA, Sep. 2019, pp. 3528–3542.
- [69] D. Borio, H. Li, and P. Closas, "Huber's non-linearity for GNSS interference mitigation," *Sensors* vol. 18, no. 7, 2018, Art. no. 2217.
- [70] P. Bolla, J. Vilà-Valls, P. Closas, and E. S. Lohan, "Centralized dynamics multi-frequency GNSS carrier synchronization," *Navigation*, vol. 66, no. 3, pp. 485–504, 2019.
- [71] J. Vilà-Valls, M. Navarro, P. Closas, and M. Bertinelli, "Synchronization challenges in deep space communications," *IEEE Aerosp. Electron. Syst. Mag.*, vol. 34, no. 1, pp. 16–27, Jan. 2019.
- [72] H. Li, D. Medina, J. Vilà-Valls, and P. Closas, "Robust Kalman filter for RTK positioning under signal-degraded scenarios," in *Proc. 32nd Int. Tech. Meeting Satellite Division Inst. Navigation*, Miami, FL, USA, Sep. 2019, pp. 16–20.
- [73] D. Dardari, P. Closas, and P. M. Djurić, "Indoor tracking: Theory, methods, and technologies," *IEEE Trans. Veh. Technol.*, vol. 64, no. 4, pp. 1263–1278, Apr. 2015.
- [74] O. Montenbruck and P. Ramos-Bosch, "Precision real-time navigation of LEO satellites using global positioning system measurements," *GPS Solutions*, vol. 12, no. 3, pp. 187–198, Jul. 2008.
- [75] S. K. Biswas and H. B. Hablani, "Ground based navigation of spacecraft in lunar transfer trajectory, with application to Chandrayaan-2," in *Advances in Estimation, Navigation, and Spacecraft Control*, D. Choukroun, Y. Oshman, J. Thienel, and M. Idan, Eds. Berlin, Germany: Springer, pp. 371–390, 2015.

- [76] S. K. Biswas, L. Qiao, and A. G. Dempster, "A novel a priori state computation strategy for the unscented Kalman filter to improve computational efficiency," *IEEE Trans. Autom. Control*, vol. 62, no. 4, pp. 1852–1864, Apr. 2017.
- [77] S. K. Biswas, L. Qiao, and A. G. Dempster, "Computationally efficient unscented Kalman filtering techniques for launch vehicle navigation using a spaceborne GPS receiver," in *Proc. 29th Int. Tech. Meeting Satellite Division Instit. Navigation*, Portland, OR, USA, 2016.
- [78] S. K. Biswas and A. G. Dempster, "Approximating sample state vectors using the ESPT for computationally efficient particle filtering," *IEEE Trans. Signal Process.*, vol. 67, no. 7, pp. 1918–1928, Apr. 2019.
- [79] P. Closas and A. Gusi-Amigó, "Direct position estimation of GNSS Receivers: Analyzing main results, architectures, enhancements, and challenges," *IEEE Signal Process. Mag.*, vol. 34, no. 5, pp. 72–84, Sep. 2017.
- [80] P. Closas and C. Fernández-Prades, "Bayesian nonlinear filters for direct position estimation," in *Proc. IEEE Aerosp. Conf.*, Big Sky, MT, USA, Mar. 2010, pp. 1–12.
- [81] P. Closas *et al.*, "Evaluation of GNSS direct position estimation in realistic multipath channels," in *Proc. 28th Int. Tech. Meeting Satellite Division Instit. Navigation*, Tampa, FL, USA, Sep. 2015, pp. 3693–3701.
- [82] A. Gusi-Amigó, P. Closas, A. Mallat, and L. Vandendorpe, "Ziv–Zakai bound for direct position estimation," *Navigation*, vol. 65, no. 3, pp. 463–475, 2018.
- [83] J. Dampf, C. A. Lichtenberger, and T. Pany, "Probability analysis for Bayesian direct position estimation in a real-time GNSS software receiver," in *Proc. 32nd Int. Tech. Meeting Satellite Division Instit. Navigation*, Miami, FL, USA, Sep. 2019, pp. 3543–3566.
- [84] J. Dampf, K. Frankl, and T. Pany, "Optimal particle filter weight for Bayesian direct position estimation in a GNSS receiver," *Sensors*, vol. 18, no. 8, 2018, Art. no. 2736.
- [85] P. Teunissen, "Carrier phase ambiguity resolution," in *Springer Handbook of Global Navigation Satellite Systems*, P. Teunissen and O. Montenbruck, Eds. New York, NY, USA: Springer, 2018, pp. 661–686.
- [86] J. Kouba, F. Lahaye, and P. Tétreault, "Precise point positioning," in *Springer Handbook of Global Navigation Satellite Systems*, P. Teunissen and O. Montenbruck, Eds. New York, NY, USA: Springer, 2018, pp. 723–752.
- [87] S. Verhagen and P. Teunissen, "Least-squares estimation and Kalman filtering," in *Springer Handbook of Global Navigation Satellite Systems*, P. Teunissen and O. Montenbruck, Eds. New York, NY, USA: Springer, 2018, pp. 630–660.
- [88] J.-H. Won and T. Pany, "Signal processing," in *Springer Handbook of Global Navigation Satellite Systems*, P. Teunissen and O. Montenbruck, Eds. New York, NY, USA: Springer, 2018, pp. 401–442.
- [89] P. Teunissen and O. Montenbruck, Eds., *Springer Handbook of Global Navigation Satellite Systems*. New York, NY, USA: Springer, 2018.
- [90] Y. Sun and M. Kumar, "Nonlinear Bayesian filtering based on Fokker–Planck equation and tensor decomposition," in *Proc. 18th Int. Conf. Inf. Fusion*, Washington, DC, USA, 2015, pp. 1483–1488.
- [91] M. A. Khan, M. Ulmke, B. Demissie, F. Govaers, and W. Koch, "Combining log-homotopy flow with tensor decomposition based solution for Fokker–Planck equation," in *Proc. 19th Int. Conf. Inf. Fusion*, Istanbul, Turkey, 2016.
- [92] F. Govaers, B. Demissie, M. A. Khan, M. Ulmke, and W. Koch, "Tensor decomposition-based multitarget tracking in cluttered environments," *J. Adv. Inf. Fusion*, vol. 14, no. 1, pp. 86–97, Sep. 2017.
- [93] D. F. Crouse, "The Tracker Component Library: Free routines for rapid prototyping," *IEEE Aerosp. Electron. Syst. Mag.*, vol. 32, no. 5, pp. 18–27, May 2017.
- [94] M. Šimandl and J. Královec, "Filtering, prediction and smoothing with Gaussian sum representation," in *Proc. 12th IFAC Symp. Syst. Identification*, Santa Barbara, CA, USA, 2020, pp. 1157–1162.
- [95] V. E. Beneš, "Exact finite-dimensional filters for certain diffusions with nonlinear drift," *Stochastics*, vol. 5, pp. 65–92, 1981.
- [96] F. E. Daum, "Exact finite-dimensional nonlinear filters," *IEEE Trans. Autom. Control*, vol. 31, no. 7, pp. 616–622, Jul. 1986.
- [97] R. Kulhavý, *Recursive Nonlinear Estimation: A Geometric Approach*. New York, NY, USA: Springer-Verlag, 1996.
- [98] G. Evensen, *Data Assimilation: The Ensemble Kalman Filter*, 2nd ed. New York, NY, USA: Springer, 2009.
- [99] A. Bouchard-Côté, S. J. Vollmer, and A. Doucet, "The bouncy particle sampler: A nonreversible rejection-free Markov chain Monte Carlo method," *J. Amer. Statist. Assoc.*, vol. 113, no. 522, pp. 855–867, 2018.
- [100] D. F. Crouse, "Particle flow filters: Biases and bias avoidance," in *Proc. 22nd Int. Conf. Inf. Fusion*, Ottawa, ON, Canada, 2019.
- [101] S. S. Blackman, "Multiple hypothesis tracking for multiple target tracking," *IEEE Aerosp. Electron. Syst. Mag.*, vol. 19, no. 1, pp. 5–18, Jan. 2004.
- [102] B. Vo, S. S. Singh, and A. Doucet, "Sequential Monte Carlo methods for multi-target filtering with random finite sets," *IEEE Trans. Aerosp. Electron. Syst.*, vol. 41, no. 4, pp. 1224–1245, Oct. 2005.
- [103] B. Vo and W. K. Ma, "The Gaussian mixture probability hypothesis density filter," *IEEE Trans. Signal Process.*, vol. 54, no. 11, pp. 4091–4104, Nov. 2006.
- [104] E. Baser, T. Kirubarajan, M. Efe, and B. Balaji, "Improved multi-target multi-Bernoulli filter with modelling of spurious targets," *IET Radar, Sonar Navigation*, vol. 10, no. 2, pp. 285–298, 2016.

- [105] S. K. Biswas, "Computationally efficient non-linear Kalman filters for on-board space vehicle navigation," Ph.D. dissertation, UNSW Sydney, Sydney, Australia, 2017.
- [106] F. L. Markley, "Attitude error representations for Kalman filtering," *J. Guid., Control, Dyn.*, vol. 26, no. 2, pp. 311–317, Mar. 2003.
- [107] R. Zanetti, "Autonomous midcourse navigation for lunar return," *J. Spacecraft Rockets*, vol. 46, no. 4, pp. 865–873, Jul. 2009.
- [108] D. Woodbury and J. Junkins, "On the consider Kalman filter," in *Proc. AIAA Guid., Navigation, Control Conf.*, Toronto, ON, Canada, Aug. 2010, pp. 1–28.
- [109] A. Giannitrapani, N. Ceccarelli, F. Scortecci, and A. Garulli, "Comparison of EKF and UKF for spacecraft localization via angle measurements," *IEEE Trans. Aerosp. Electron. Syst.*, vol. 47, no. 1, pp. 75–84, Jan. 2011.
- [110] L. Zhang, T. Li, H. Yang, S. Zhang, H. Cai, and S. Qian, "Unscented Kalman filtering for relative spacecraft attitude and position estimation," *J. Navigation*, vol. 68, no. 03, pp. 528–548, 2014.
- [111] X. Ning and J. Fang, "Spacecraft autonomous navigation using unscented particle filter-based celestial/Doppler information fusion," *Meas. Sci. Technol.*, vol. 19, no. 9, Sep. 2008, Art. no. 095203.
- [112] O. Montenbruck, S. Hackel, and A. Jäggi, "Precise orbit determination of the Sentinel-3 A altimetry satellite using ambiguity-fixed GPS carrier phase observations," *J. Geodesy*, vol. 92, no. 7, pp. 711–726, Jul. 2018.
- [113] D. Gebre-Egziabher, G. H. Elkaim, J. D. Powell, and B. W. Parkinson, "A non-linear, two-step estimation algorithm for calibrating solid-state strapdown magnetometers," in *Proc. 8th Int. St. Petersburg Conf. Navigat. Syst.*, St. Petersburg, Russia, 2001.
- [114] N. El-Sheimy, H. Hou, and X. Niu, "Analysis and modeling of inertial sensors using Allan variance," *IEEE Trans. Instrum. Meas.*, vol. 57, no. 1, pp. 140–149, Jan. 2008.
- [115] J. Duník et al., "Estimation of state and measurement noise characteristics," in *Proc. 18th Int. Conf. Inf. Fusion*, Washington, DC, USA, 2015, pp. 1817–1824.